

# The conformal sector of Quantum Einstein Gravity beyond the local potential approximation

Alfio Bonanno

*INAF, Osservatorio Astrofisico di Catania, via S. Sofia 78, I-95123 Catania, Italy ;  
INFN, Sezione di Catania, via S. Sofia 64, I-95123, Catania, Italy.*

Maria Conti

*DISAT, Università degli Studi dell'Insubria, via Valleggio 11, I-22100 Como, Italy ;  
INFN, Sezione di Milano, Via Celoria 16, I-20133 Milano, Italy.*

Dario Zappalà

*INFN, Sezione di Catania, via S. Sofia 64, I-95123, Catania, Italy;  
Centro Siciliano di Fisica Nucleare e Struttura della Materia, Catania, Italy.*

arXiv:2309.15514v1 [hep-th] 27 Sep 2023

---

## Abstract

The anomalous scaling of Newton's constant around the Reuter fixed point is dynamically computed using the functional flow equation approach. Specifically, we thoroughly analyze the flow of the most general conformally reduced Einstein-Hilbert action. Our findings reveal that, due to the distinctive nature of gravity, the anomalous dimension  $\eta$  of the Newton's constant cannot be constrained to have one single value: the ultraviolet critical manifold is characterized by a line of fixed points  $(g_*(\eta), \lambda_*(\eta))$ , with a discrete (infinite) set of eigenoperators associated to each fixed point. More specifically, we find three ranges of  $\eta$  corresponding to different properties of both fixed points and eigenoperators and, in particular, the range  $\eta < \eta_c \approx 0.96$  the ultraviolet critical manifolds has finite dimensionality.

*Keywords:* Functional Renormalization Group, Asymptotic Safety

---

## 1. Introduction

Understanding the structure of the ultraviolet (UV) critical manifold in Asymptotically Safe (AS) theories of gravity has been a formidable challenge despite substantial efforts. A striking departure from well-established examples, such as scalar theories in  $d$  dimensions, lies in the unique role played by Newton's constant,  $G_N$ , in determining the scaling dimension of the gravitational field in the action:

$$S[g_{\mu\nu}] = -\frac{1}{16\pi} \int d^4x \frac{1}{G_N} \sqrt{g} R \quad (1)$$

In this context, the inverse of  $G_N$ , equivalent to the wavefunction renormalization function  $Z$  for the graviton, assumes a central role. Percacci and Perini highlighted a crucial distinction from the scalar field case, where, despite its technical inessentiality [1],  $1/G_N$  should scale as the inverse of the cut-off square. Consequently, the anomalous dimension of the field obeys the equation:

$$\eta = \beta_N - 2. \quad (2)$$

Here,  $\beta_N$  denotes the beta-function for Newton's constant which can be obtained from (1). At the fixed point (FP), where  $\beta_N$  vanishes, the anomalous dimension  $\eta$  takes on the value of  $-2$  [2–4]. The value  $\eta = -2$  merely reflects the classical (negative) natural dimension of the background Newton's constant. In contrast, the anomalous dimension associated with graviton fluctuations, denoted as  $\eta_h$ , emerges dynamically and takes a value close to one ( $\eta_h \approx 1.02$  as reported in [5]).

The central question we aim to tackle in this paper is whether we can transcend the definition provided in equation (2), which is based on a  $\beta$ -function approach, (i.e. implying polynomial truncation of the theory space), and propose a dynamic determination of the anomalous dimension of the background field, similar to the case of inessential couplings in standard quantum field theory (QFT). To overcome the limitations of equation (2), it is evident that we must approach the problem at a non-perturbative level, taking into account all possible operators compatible with the general group of diffeomorphisms.

As originally pioneered by Wilson and Wegner [6, 7], the Renormalization Group (RG), when implemented with the aid of Functional Flow Equations, serves as a powerful tool for exploring the structure of the UV critical manifold at a non-perturbative level [8–11]. At the heart of this approach lies the Effective Average Action  $\Gamma_k$ , representing the effective action

---

*Email addresses:* [alfio.bonanno@inaf.it](mailto:alfio.bonanno@inaf.it) (Alfio Bonanno),  
[mconti@uninsubria.it](mailto:mconti@uninsubria.it) (Maria Conti), [dario.zappala@ct.infn.it](mailto:dario.zappala@ct.infn.it)  
(Dario Zappalà)

of the system at the scale  $k$ , which converges to the familiar Effective Action in the limit as  $k \rightarrow 0$ .

In recent years, the Renormalization Group, implemented with Functional Flow Equations, has proven invaluable for exploring the properties of the UV critical manifold in Asymptotically Safe (AS) theories of gravity beyond the framework defined in (1). Researchers have turned to theories of the form:

$$\Gamma_k[g_{\mu\nu}] = \frac{1}{16\pi} \int d^d x \sqrt{g} f_k(R), \quad (3)$$

aiming to move beyond polynomial truncation. For an extensive review of this approach, please refer to [12]. The rationale behind (3) draws parallels with the Local Potential Approximation (LPA) in scalar theories, where exact flow equations for the potential  $V(\phi)$  have been derived and successfully solved, leading to highly accurate studies of critical properties in dimensions  $d = 3$  and  $d = 4$ . Despite substantial computational efforts dedicated to analyzing scaling solutions (i.e., fixed point) of the flow equation for (3), progress in moving beyond Eq. (2) has remained somewhat limited. This challenge is further compounded by the issue of background independence.

The Wetterich equation is grounded in the Effective Average Action  $\Gamma_k$ , which, in the context of the background field method, depends on two distinct metrics: the full metric  $g_{\mu\nu}$  and the background field metric  $\bar{g}_{\mu\nu}$ . While in standard gauge theory all correlation functions of the fundamental field can be derived from “on shell” background field correlation functions with the aid of a gauge-fixing term invariant under a background transformation, in gravity, particularly following the tenets of loop quantum gravity [13], background independence carries a more profound significance. Here, full background independence entails that no metric should hold any privileged status at any stage of the calculation.

Given the formidable technical complexity of achieving full background independence, advancement in this direction necessitates significant simplifications. For instance, building upon the approach initiated by [14, 15], several studies have explored a conformally reduced version of the theory [16, 17], demonstrating that the conformal factor plays a pivotal role in generating the Reuter fixed point with a finite number of relevant directions, even beyond the standard Einstein-Hilbert truncation [18].

In contrast, Morris and his collaborators have addressed the more rigorous requirement of full background independence directly within the flow equation framework in a series of works [19–21]. Particularly, in [21], the use of a specific cutoff function allowed for the examination of the ultraviolet critical manifold of the conformally reduced theory beyond the LPA approximation employed in [15]. A significant finding from this work is the identification of a line of fixed points, each with a continuous set of relevant eigendirections. Taken at face value, this result suggests that the theory is renormalizable but not predictive, given the infinite number of relevant directions.

In this paper, we pursue an alternative path. We employ a spectrally-adjusted cutoff [22] previously utilized in scalar theory and quantum gravity investigations [17, 23, 24], to surpass the LPA approximation presented in [15]. Consequently, we

adopt a single metric approximation for the renormalized flow. By virtue of our cutoff selection, we are able to obtain analytical solutions. While we confirm the presence of a line of fixed points, we observe a discrete spectrum of eigendirections. Notably, the UV critical manifold exhibits finite dimensionality for  $\eta < \eta_c \approx 0.96$ .

The structure of the paper is the following. In Sec. 2 the general framework and the approximation scheme are discussed; in Sec. 3 the numerical analysis employed for the determination of the fixed points and for the eigenvalue spectra is presented; the conclusions are reported in Sec. 4.

## 2. General setup and differential equations in the flat projection

We start by considering the well known Euclidean Einstein-Hilbert action [17]

$$S^{EH}[g_{\mu\nu}] = -\frac{1}{16\pi} \int d^d x \sqrt{g} G^{-1} (R - 2\Lambda), \quad (4)$$

which, by Weyl rescaling  $g_{\mu\nu} = \phi^{2\nu} \hat{g}_{\mu\nu}$  where  $\nu$  is a parameter taken as  $\nu = \frac{2}{d-2}$ , can be written as

$$S_k^{EH}[\phi] = \int d^d x \frac{\sqrt{\hat{g}} Z_k}{2} \left( \hat{g}^{\mu\nu} \partial_\mu \phi \partial_\nu \phi + A \hat{R} \phi^2 - 4A \Lambda_k \phi^{\frac{2d}{d-2}} \right), \quad (5)$$

where  $\hat{R} \equiv R(\hat{g})$ ,  $A = A(d) = \frac{d-2}{8(d-1)}$  and

$$Z_k = -\frac{1}{2\pi G_k} \frac{d-1}{d-2} \quad (6)$$

and it is assumed that  $\Lambda_k$  and  $G_k$  (and  $Z_k$  through Eq. (6)) are RG scale  $k$ -dependent parameters. It is then convenient to consider a general action of the type

$$S_k[\phi] = \int d^d x \sqrt{\hat{g}} \left( \frac{1}{2} Z_k \hat{g}^{\mu\nu} \partial_\mu \phi \partial_\nu \phi + V_k[\phi] \right), \quad (7)$$

where  $V_k[\phi] \equiv Z_k U_k[\phi]$ , with  $U[\phi]$  a potential term for the action. Then, the parallel between Eqs. (5) and (7) is evident.

Following [17, 23] the proper-time flow equation reads

$$\partial_t \Gamma_k[f; \chi_B] = -\frac{1}{2} \text{Tr} \int_0^\infty \frac{ds}{s} \partial_t \rho_k \exp \left( -s \frac{\delta^2 \Gamma_k[f; \chi_B]}{\delta f^2} \right), \quad (8)$$

where  $t \equiv \log k$  is the RG time and the original field  $\phi$  is split into a constant background component  $\chi_B$  and a dynamical fluctuation  $\bar{f}$ :  $\phi(x) = \chi_B + \bar{f}(x)$ . Moreover, a reference metric  $\hat{g}_{\mu\nu}$  is chosen through a Weyl rescaling  $\bar{g}_{\mu\nu} = \chi_B^{2\nu} \hat{g}_{\mu\nu}$ , with constant  $\chi_B$  and  $\nu = 2/(d-2)$ , where  $d$  is the space-time dimension and, because of this definition, the two momenta scales (defined as the Eigenvalues of the  $-\hat{\square}$  and  $-\bar{\square}$  respectively) are usually related through

$$\hat{k}^2 = \chi_B^{2\nu} \bar{k}^2. \quad (9)$$

and the conformal factor is considered as dimensionless. However, as discussed in the introduction, in our investigation we consider an anomalous scaling for the  $\chi_B$  and we write

$$\chi_B = \psi_B k^{\frac{\eta}{2}}. \quad (10)$$

being  $\psi_B$  a dimensionless field and  $\eta$  the anomalous dimension. This choice entails some differences with respect to (9). While the identity  $\hat{\square} = \chi_B^{2\nu} \bar{\square}$  always holds true, in order for  $\hat{\square}$  to show the correct dimensionality of  $k^2$  ( $[\hat{\square}] = k^2$ ), it must imply:  $[\bar{\square}] = k^{2-\eta\nu}$ . Hence, the relation between momenta built with the reference metric and the background metric must be of the following form:

$$\hat{k}^2 = \chi_B^{2\nu} \bar{k}^{2-\eta\nu}, \quad (11)$$

which for  $d = 4$ , i.e.  $\nu = 1$ , simply reduces to  $\hat{k}^2 = \chi_B^2 \bar{k}^{2-\eta}$ . The smooth infrared (IR) regulator  $\rho_k = \rho_k[\chi_B]$  (repeatedly analyzed in the literature [17, 22–26]), which depends on the background field only  $\chi_B$ , and whose role is to restrict the integration to the modes with  $p \geq k$ , is taken as in [17]: because of the new relation (11), it now assumes the form

$$\partial_t \rho_k(s, n) = -\frac{2}{\Gamma(n)} (s n Z_k k^{2-\eta\nu} \chi_B^{2\nu})^n e^{-s n Z_k k^{2-\eta\nu} \chi_B^{2\nu}}, \quad (12)$$

where  $n$  is a positive integer number controlling the sharpness of the cutoff and  $\Gamma(n)$  is the Gamma function. Following the background field method, the trace must always be performed on the modes constructed with the background metric  $\bar{g}_{\mu\nu}$ , i.e. the trace must be taken on the spectrum of  $-\bar{\square}$  [14, 15]. The spectral adjustment represented by the presence of the renormalization function  $Z_k$  inside the exponential allows to correctly perform a cut on the eigenvalues of the operator  $-\hat{\square}$  when the original theory contains corrected operators of the type  $-Z_k \hat{\square}$ .

The implementation in Eq. (7) of an expansion in powers of the field fluctuation

$$\bar{f} = \phi(x) - \chi_B \quad (13)$$

around the constant background  $\chi_B$ , leads to the following form for the left hand side of the flow equation:

$$\partial_t \Gamma_k = \int d^d x \sqrt{\bar{g}} \left( \frac{1}{2} (k \partial_k Z_k) [\chi_B] \bar{f} \hat{\square} \bar{f} + k \partial_k V_k [\chi_B] \right). \quad (14)$$

The right hand side of the flow equation can instead be expressed as

$$-\frac{1}{2} \int \frac{ds}{s} \int d^d x \sqrt{\bar{g}} \int \frac{d^d \bar{p}}{(2\pi)^d} (k \partial_k \rho_k) \langle x | \bar{p} \rangle \langle \bar{p} | e^{-s \Gamma_k^{(2)}} | x \rangle, \quad (15)$$

where the trace is performed on the modes of  $-\bar{\square}$ . This expression can be expanded through Baker-Campbell-Hausdorff expansion up to quadratic terms in  $\bar{f}$ , leading to

$$-\frac{1}{2} \int \frac{ds}{s} \int d^d x \chi_B^{d\nu} \sqrt{\bar{g}} (k \partial_k \rho_k) \int \frac{d^d \bar{p}}{(2\pi)^d} e^{-s(Z_k \chi_B^{2\nu} \bar{p}^{2-\eta\nu} + V_k^{(2)})} \times \left( 1 - s B_1 + \frac{s^2}{2!} B_2 - \frac{s^3}{3!} B_3 + \frac{s^4}{4!} B_4 \right) \quad (16)$$

where the identity  $\sqrt{\bar{g}} = \chi_B^{d\nu} \sqrt{\hat{g}}$  was inserted. The expressions denoted with  $B_i$  with  $i = 1, 2, 3, 4$  explicitly read

$$B_1 = \left[ Z'[\chi_B] \hat{p}^2 \bar{f} + \frac{Z''[\chi_B]}{2} \hat{p}^2 \bar{f}^2 - \frac{Z''[\chi_B]}{2} \bar{f} \hat{\square} \bar{f} + \bar{f} V^{(3)}[\chi_B] + \frac{\bar{f}^2}{2} V^{(4)}[\chi_B] \right] \Big|_{\hat{\square} = \chi_B^{2\nu} \bar{\square}, \hat{p}^2 = \chi_B^{2\nu} \bar{p}^{2-\eta\nu}}; \quad (17)$$

$$B_2 = \left[ (Z'[\chi_B])^2 \hat{p}^4 \bar{f}^2 - (Z'[\chi_B])^2 \left( 2 + \frac{1}{d} \right) \hat{p}^2 \bar{f} \hat{\square} \bar{f} + 2Z'[\chi_B] V^{(3)}[\chi_B] \hat{p}^2 \bar{f}^2 - 2Z'[\chi_B] V^{(3)}[\chi_B] \bar{f} \hat{\square} \bar{f} + \bar{f}^2 (V^{(3)}[\chi_B])^2 \right] \Big|_{\hat{\square} = \chi_B^{2\nu} \bar{\square}, \hat{p}^2 = \chi_B^{2\nu} \bar{p}^{2-\eta\nu}}; \quad (18)$$

$$B_3 = \left[ -Z[\chi_B] (Z'[\chi_B])^2 \left( 1 + \frac{4}{d} \right) \hat{p}^4 \bar{f} \hat{\square} \bar{f} - Z[\chi_B] Z'[\chi_B] V^{(3)}[\chi_B] \left( 2 + \frac{4}{d} \right) \hat{p}^2 \bar{f} \hat{\square} \bar{f} - Z[\chi_B] (V^{(3)}[\chi_B])^2 \bar{f} \hat{\square} \bar{f} \right] \Big|_{\hat{\square} = \chi_B^{2\nu} \bar{\square}, \hat{p}^2 = \chi_B^{2\nu} \bar{p}^{2-\eta\nu}}; \quad (19)$$

$$B_4 = \left[ -(Z[\chi_B])^2 (Z'[\chi_B])^2 \frac{4}{d} \hat{p}^6 \bar{f} \hat{\square} \bar{f} - (Z[\chi_B])^2 Z'[\chi_B] V^{(3)}[\chi_B] \frac{8}{d} \hat{p}^4 \bar{f} \hat{\square} \bar{f} - (Z[\chi_B])^2 (V^{(3)}[\chi_B])^2 \frac{4}{d} \hat{p}^2 \bar{f} \hat{\square} \bar{f} \right] \Big|_{\hat{\square} = \chi_B^{2\nu} \bar{\square}, \hat{p}^2 = \chi_B^{2\nu} \bar{p}^{2-\eta\nu}}. \quad (20)$$

As already discussed, in Eqs. (17)-(20) the two relations  $\hat{\square} = \chi_B^{2\nu} \bar{\square}$  and  $\hat{p}^2 = \chi_B^{2\nu} \bar{p}^{2-\eta\nu}$  are enforced. The latter was also applied to the momenta appearing in Eq. (12), which specifies the form of the regulator. After integrating over the background momenta  $\bar{p}$  and over the variable  $s$  in (16), a comparison with the left hand side of the flow equation in (14) allows to identify the flow equations for  $V_k$  and  $Z_k$ . Apart from a common coefficient  $C$

$$C = \frac{2^{-d} \pi^{-d/2} \Gamma\left(\frac{d-\eta\nu+2}{2-\eta\nu}\right) n^{\frac{d}{2-\eta\nu}} \Gamma\left(\frac{d}{\eta\nu-2} + n\right)}{\Gamma\left(\frac{d}{2} + 1\right) \Gamma(n)}, \quad (21)$$

the dimensional equations (with general dimension  $d$  and shaping parameter  $n$ ) for  $V_k$  and  $Z_k$  are:

$$\partial_t V_k = n^{\frac{d}{f_0} + n} \psi^{d\nu} k^{-f_0 n} W_1^{-\frac{d}{f_0} - n} Z_k^{\frac{d}{f_0} + n} \chi_B^{2\nu \left(\frac{d}{f_0} + n\right)} \quad (22)$$

and

$$\partial_t Z_k = -\frac{1}{3f_0^4} q_0 n^{\frac{d}{f_0} + n} Z_k^{\frac{d}{f_0} + n - 1} k^{\frac{\eta\nu(d+f_0)}{f_0} + 2n} \chi_B^{\frac{2\nu(d+n f_0 - 4)}{f_0}} \psi^{d\nu} W_2^{-\frac{d+f_0(n+3)}{f_0}} \times \left( \chi_B^{\frac{8\nu}{f_0}} k^{2n\nu} (V_k''^2 (3f_0^3 Z_k Z_k'' + u_0 Z_k'^2) + r_0 V_k^{(3)} Z((f_0 + 1)s_0 V_k^{(3)} Z_k - 2t_0 V_k'' Z_k') + -2n Z_k k^l_0 \chi_B^{\frac{2l_0\nu}{f_0}} (r_0 t_0 V_k^{(3)} Z_k Z_k' - V_k'' (3f_0^3 Z_k Z_k'' + u_0 Z_k'^2)) + + k^4 n^2 Z_k^2 \chi_B^{\frac{4m_2\nu}{f_0}} (3f_0^3 Z_k Z_k'' + u_0 Z_k'^2) \right), \quad (23)$$

where the derivatives are taken with respect to the field  $\phi$ . Inside (22) and (23), the following quantities have been introduced for brevity:

$$W_1 = n Z_k \chi_B^{2\nu} k^{2-\eta\nu} + V_k'' \quad (24)$$

$$W_2 = k^2 n Z_k \chi_B^{2\nu} + k^{\eta\nu} V_k'' \quad (25)$$

Together with  $W_1$  and  $W_2$ , the functions  $f_0$ ,  $g_0$ ,  $h_0$  and  $l_0$  have been defined as  $f_0 = \eta\nu - 2$ ,  $g_0 = 3\eta\nu - 5$ ,  $h_0 = 5\eta\nu - 9$  and  $l_0 = 2 + \eta\nu$ , that appear in the following definitions

$$q_0 = d + f_0 n \quad (26)$$

$$r_0 = d + f_0(1 + n) \quad (27)$$

$$s_0 = d + f_0(2 + n) \quad (28)$$

$$t_0 = d(1 + f_0) + f_0 g_0 \quad (29)$$

$$u_0 = d^2(f_0 + 1) + d f_0 h_0 + f_0^2 \quad (30)$$

and the '0' subscripts have been introduced to avoid confusion with other variables. We now introduce  $Y_k$ ,  $z_k$ ,  $X$  as the dimensionless counterparts of the potential  $V_k$ , the renormalization function  $Z_k$  and the field  $\phi$  respectively as follows:

$$V_k[\phi] = Y_k[X]k^d \quad (31)$$

$$Z_k[\phi] = z_k[X]k^{d-2-\eta} \quad (32)$$

$$\phi = X k^{\frac{\eta}{2}}, \quad (33)$$

where  $\eta$  represents the anomalous dimension of *both* fields  $\chi_B$  and  $\phi$ , as shown by equations (10) and (33) respectively.

Following the single field approximation [17], once the fluctuation  $\bar{f}$  defined in (13) is integrated out, the expectation value of the dimensionless field  $X$ , introduced in Eq. (33), is identified with the background  $\psi_B$ , which, for the sake of simplicity, from now on is indicated as  $x$ :

$$X = \psi_B \equiv x. \quad (34)$$

In terms of the dimensionless quantities  $Y_k$  and  $z_k$  in  $d = 4$ , equations (22) and (23) now read more easily as:

$$\partial_t Y_k(x) = -4Y_k + \frac{\eta x Y'_k}{2} + n \frac{4}{\eta-2} + 2n \frac{10\eta}{x^{\frac{4}{\eta-2}+2n}} z_k^{\frac{4}{\eta-2}+n} Q_1^{-\frac{4}{\eta-2}-n-3} Q_2^3 \quad (35)$$

and

$$\begin{aligned} \partial_t z_k(x) = & (\eta - 2)z_k + \frac{\eta x z'_k}{2} - \frac{n \frac{4}{\eta-2} + n ((\eta - 2)n + 4) \frac{4\eta}{x^{\frac{4}{\eta-2}+2n}} \times}{3(\eta - 2)^4} \\ & \times z_k^{\frac{4}{\eta-2}+n-1} Q_1^{-\frac{4}{\eta-2}-n-3} \left\{ (\eta - 1)(Y_k^{(3)})^2 z_k^2 ((\eta - 2)(n + 1) + 4) \times \right. \\ & \times ((\eta - 2)(n + 2) + 4) - (4(\eta - 1) + (\eta - 2)(3\eta - 5)) \times \\ & \times ((\eta - 2)(n + 1) + 4) 2 Y_k^{(3)} z_k z'_k Q_1 + [3(\eta - 2)^3 z_k z'_k + \\ & \left. + ((\eta - 2)^2 + 4(5\eta - 9)(\eta - 2) + 16(\eta - 1))(z'_k)^2 \right] Q_1^2 \} \quad (36) \end{aligned}$$

where

$$Q_1 = (n x^2 z_k + Y_k'') \quad (37)$$

and

$$Q_2 = \left( n x^{-\frac{4}{\eta-2}} z_k + x^{-\frac{2\eta}{\eta-2}} Y_k'' \right) \quad (38)$$

and the derivatives appearing in the right hand side of (35) and (36) are taken with respect to the dimensionless field  $X$ .

Eqs. (35) and (36) are lengthy and rather involved as far as their numerical treatment is concerned, especially in the case of large  $n$ . Therefore we shall take the limit  $n \rightarrow +\infty$  in the two flow equations, which are turned into a more compact form, as

all the troublesome powers of  $n$  in (35) and (36) are replaced in this limit by  $n$ -independent exponential factors that are easier to handle numerically. In this limit, the two flow equations read:

$$\partial_t Y_k(x) = -4Y_k + \frac{1}{2}\eta x Y'_k + x^4 e^{-\frac{Y_k}{x^2 z_k}} \quad (39)$$

and

$$\begin{aligned} \partial_t z_k(x) = & (\eta - 2)z_k + \frac{1}{2}\eta x z'_k - \frac{e^{-\frac{Y_k}{x^2 z_k}}}{3(\eta - 2)^3 x^2 z_k^2} \times \\ & \times \left[ (\eta - 2)^2 (\eta - 1) (Y_k^{(3)})^2 + \right. \\ & + 2(-3\eta^3 + 13\eta^2 - 20\eta + 12) x^2 Y_k^{(3)} z'_k + \\ & \left. + x^4 (3(\eta - 2)^3 z_k z'_k + (21\eta^2 - 64\eta + 60)(z'_k)^2) \right] \quad (40) \end{aligned}$$

In the next Section we shall analyse the fixed point structure of these flow equations including the central role of the anomalous dimension  $\eta$  and then, the nature of the related eigendirections.

### 3. The role of the anomalous dimension

#### 3.1. The fixed point line structure

In this Section we focus on the fixed point solutions of the flow equations (39) and (40), i.e.  $\partial_t Y_k(x) = \partial_t z_k(x) = 0$ , for the generalization of the conformally reduced Einstein- Hilbert (CREH) truncation shown in (5), with  $d = 4$  and with flat curvature  $\hat{R} = 0$ . It is easy to check that the functions

$$z = -\frac{1}{w} \quad (41)$$

$$Y = \frac{u}{w} x^4 \quad (42)$$

(where  $w$  and  $u$  are numerical coefficients), are such that all dependence on  $x$  gets canceled both in Eqs. (39) and (40), so that the two differential equations reduce to simple numerical equations. In addition, from (4), (5), (6) and (41), (42), one easily deduce that  $u$  and  $w$  correspond respectively to the dimensionless cosmological constant  $\lambda$  and Newton's constant  $g$ .

It is crucial to remark that all numerical searches performed to determine alternative solutions  $Y(x)$  and  $z(x)$  did not produce any positive result, leaving the monomial functions in (41) and (42) as the only acceptable fixed point solution among the entire set of real, polynomial or non-polynomial, functions.

After replacing the functions (41), (42) in Eqs. (39) and (40), we get the following equations in terms of the three parameters  $u$ ,  $w$ , and  $\eta$ :

$$e^{12u} + \frac{2u(-2 + \eta)}{w} = 0 \quad (43)$$

$$\frac{2 - \eta}{w} - \frac{192 e^{12u} u^2 (-1 + \eta)}{-2 + \eta} = 0 \quad (44)$$

Clearly, one of the three parameters cannot be determined and we choose to parameterize the solutions of Eqs. (43), (44), in terms of the anomalous dimension  $\eta$ . The corresponding solutions  $u^*(\eta)$  and  $w^*(\eta)$  are reported in Fig. 1. It is evident from Eqs. (43), (44), that  $\eta = 2$  is a singular point, whose origin can

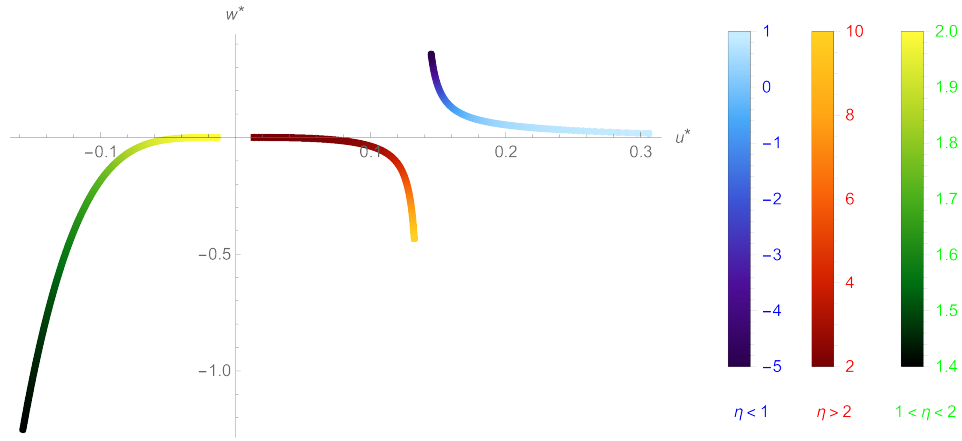


Figure 1: Fixed point line for different values of the anomalous dimension  $\eta$ .  
 Blue curve:  $\eta < 1$ ; red curve:  $\eta > 2$ ; green curve:  $1 < \eta < 2$ .

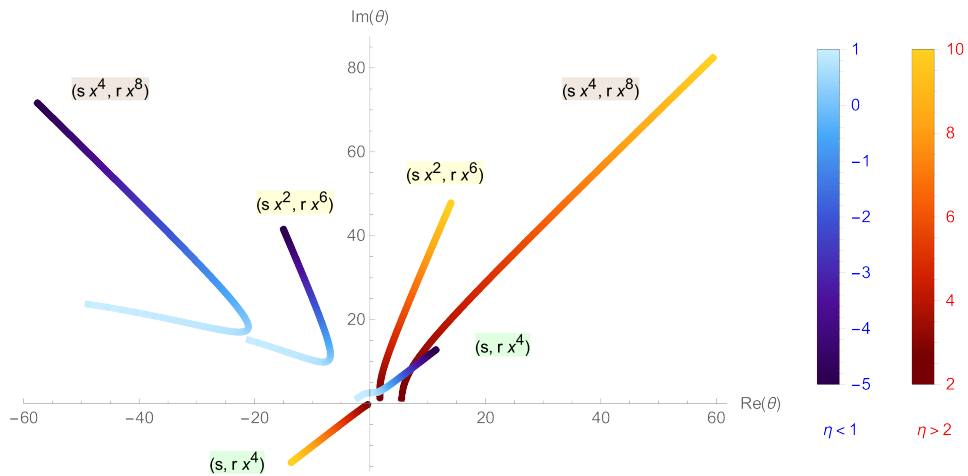


Figure 2: Eigenvalues for three different types of eigenfunctions:  $(f, h) = \{(s, r x^4), (s x^2, r x^6), (s x^4, r x^8)\}$ , for different values of the anomalous dimension  $\eta$ . Blue curve:  $\eta < 1$ ; red curve:  $\eta > 2$ . As eigenvalues always show the form  $\theta_{1,2} = \text{Re}(\theta) \pm i \text{Im}(\theta)$  for these values of  $\eta$ , only one of the two Eigenvalues is plotted.

be traced back to the dimensions of the background field and to the exponent of the momentum  $\bar{k}$  in Eq. (11). However, as can be checked in Eqs. (43) and (44),  $u^*$  and  $w^*$  are both regular and vanish in the limit  $\eta \rightarrow 2$  (In Fig. 1,  $u^*$  and  $w^*$  are plotted up to  $\eta = 2 \pm 0.001$ ). From Eqs. (43), (44), we also notice that, in the limit  $\eta \rightarrow 1$ , at least one of the two solutions  $u^*$  and  $w^*$  diverge, thus making the point  $\eta = 1$  singular; in addition, when  $\eta \rightarrow \pm\infty$ , the parameter  $w^*$  diverges.

Therefore, Fig. 1 shows three disconnected lines of fixed points parameterized in terms of the continuous variable  $\eta$ , with two singular points at  $\eta = 1$  and  $\eta = 2$ . This is quite different from the picture of a simple scalar quantum field theory where, in the same kind of analysis, one can constrain  $w^* = 1$ , because any rescaling of  $w^*$  would imply a physically irrelevant rescaling of  $u^*$  and of the field, with no change in the spectrum of the eigenvalues of the linearized flow equations around the fixed point solution. In this case, the inclusion of the same anomalous dimension for *both* fields  $\phi$  and  $\chi_B$ , together with the identification of  $u^*$  and  $w^*$  with the physically meaningful quantities  $\lambda^*$  and  $g^*$  makes the rescaling of  $w^*$  an appreciable operation. We conclude that each FP of the lines in Fig. 1, corresponds to a distinct solution.

From Fig. 1, we notice that the solutions  $u^*$  and  $w^*$  maintain a definite sign within each of the three ranges  $\eta < 1$ ,  $1 < \eta < 2$  and  $2 < \eta$ , but they can switch sign when passing from one range to another. Finally, we recall that the point  $\eta = 0$  corresponds to the usual formalism of literature [17], as (31) and (32) reproduce the known scaling of  $V_k$  and  $Z_k$ . In other words,  $\eta = 0$  must correctly reproduce the Reuter FP as in [17], characterized by  $g^* > 0$  and  $\lambda^* > 0$  and, in fact, within our computation, the Reuter FP with  $\eta = 0$  is located at  $w^* = 0.086$  and  $u^* = 0.173$ .

Although it seems natural to expect  $u^*, w^* > 0$ , which in our computation is recovered only when  $\eta < 1$ , we do not have any argument to reject the negative solutions as long as they correspond to UV fixed points whose outgoing trajectories lead in the IR limit to physically acceptable positive values of  $\lambda$  and  $g$ . Therefore the following mandatory step is the study of the eigenfunction spectrum of our flow equations.

### 3.2. Eigenfunction spectrum

The set of eigenfunctions, that stems from the resolution of the flow equations suitably linearized around a FP, determines the renormalization properties of the model at that FP. In fact, as discussed in [27], after establishing the critical surface around the FP, spanned by the full set of UV-attractive, or relevant, directions, the continuum limit of the model is realized on the ‘renormalized trajectories’ (RTs), i.e. RG flow trajectories, which land on the critical surface in the continuum limit  $t \rightarrow \infty$ . The form of the effective action in terms of eigenfunctions around a fixed point is

$$S_k[\phi] = S_*[\phi] + \sum_{i=1}^n \alpha_i e^{-\theta_i t} O_i[\phi], \quad (45)$$

where  $S_*[\phi]$  is the FP action and the operators  $O_i[\phi]$  are the eigenperturbations and  $\theta_i$  the corresponding eigenvalues. The

sign of  $\theta_i$  defines the nature of the eigenfunction, namely positive, negative or vanishing  $\theta_i$  correspond respectively to relevant, irrelevant or marginal operators. To explicitly determine the eigenvalues we express the variables  $Y(x, t)$  and  $z(x, t)$  as

$$Y(x, t) = Y^*(x) + \delta e^{-t\theta} h(x), \quad (46)$$

$$z(x, t) = z^*(x) + \delta e^{-t\theta} f(x). \quad (47)$$

where  $h(x)$  and  $f(x)$  represent small perturbations around the FP solution  $Y^*, z^*$  (which are related to  $u^*, w^*$  through Eqs. (41), (42)) and  $\delta$  is a small number used to parametrize the expansion around the FP. Remarkably, as we already found out in the case of the FP, for a specific monomial form of  $f(x)$  and  $h(x)$ , the linearized flow equations become field independent and the problem is again reduced to a set of algebraic equations.

In fact, we consider  $f(x) = s x^p$  and  $h(x) = r x^q$ , with non-negative integers  $p$  and  $q$  and with constant  $s$  and  $r$ . Then, with these prescriptions, the linearized equations (39) and (40) (i.e. the coefficients of the linear terms in  $\delta$  when Eqs. (39) and (40) are expanded in powers of  $\delta$ , after the insertion of Eqs. (46), (47)) become

$$4 - \frac{\eta q}{2} - e^{12u^*} w^* \left( \frac{12 s u^* x^{-q+p+4}}{r} + (q-1)q \right) = \theta \quad (48)$$

$$\frac{16(\eta-1)(q-1)qr e^{12u^*} u^* w^* (q+12u^*-2)x^{q-p-4}}{(\eta-2)s} + \left[ 384(\eta-2)(\eta-1)(u^*)^2(6u^*+1) + 16(\eta(3\eta-7)+6)pu^* + (\eta-2)^2p - (\eta-2)^2p^2 \right] \frac{e^{12u^*} w^*}{(\eta-2)^2} - 2 - \frac{\eta}{2}(p+2) = \theta \quad (49)$$

Only if  $q = p + 4$  these two equations become independent of  $x$  and therefore, the spectrum of eigenfunctions consists of the pairs  $(f, h) = (s, r x^4)$ ,  $(f, h) = (s x^2, r x^6)$ ,  $(f, h) = (s x^4, r x^8)$  and so on, where the coefficient  $s$  and  $r$  have to be determined separately for each eigenfunction from Eqs. (48) and (49).

Then, for each value of  $\eta$ , which selects a FP solution  $u^*(\eta)$ ,  $w^*(\eta)$  according to Fig. 1, and for each eigenfunction  $(f, h)$  we compute the parameters  $s$  and  $\theta$  from Eqs. (48) and (49) (note that in these equations the parameter  $r$  only appears in the ratio  $(s/r)$  and therefore we can choose  $r = 1$  to normalize the eigenfunction  $(f, h)$ ), whose non-linear structure provides either a pair of complex conjugate eigenvalues  $\theta, \theta^*$ , or a pair of real eigenvalues  $\theta_1, \theta_2$ . Numerous eigenfunctions were tested, up to  $(f, h) = (s x^{1000}, r x^{1004})$ , and in all cases the complex eigenvalues are found in the ranges  $\eta < 1$  and  $2 < \eta$ , while the real eigenvalues in the interval  $1 < \eta < 2$ . These results are summarized in Figs. 2, 3.

In Fig. 2 the real and imaginary part of  $\theta$  corresponding to  $\eta < 1$  (in blue), and to  $2 < \eta$  (in red), are plotted, for the three eigenfunctions corresponding to  $q = 4, 6, 8$  (we recall that the second solution for each value of  $\eta$  is  $\theta^*$ ).

We observe that the eigenvalues associated with  $q = 4$  are different from all the others as they have negative real part (which indicates irrelevant eigenfunctions) when  $2 < \eta$  and  $0.96 \simeq \eta_c < \eta < 1$ , and positive real part (relevant eigenfunctions) for  $\eta < \eta_c$ . Conversely, all other cases with  $q > 4$  show negative real part for  $\eta < 1$ , and positive for  $2 < \eta$ .

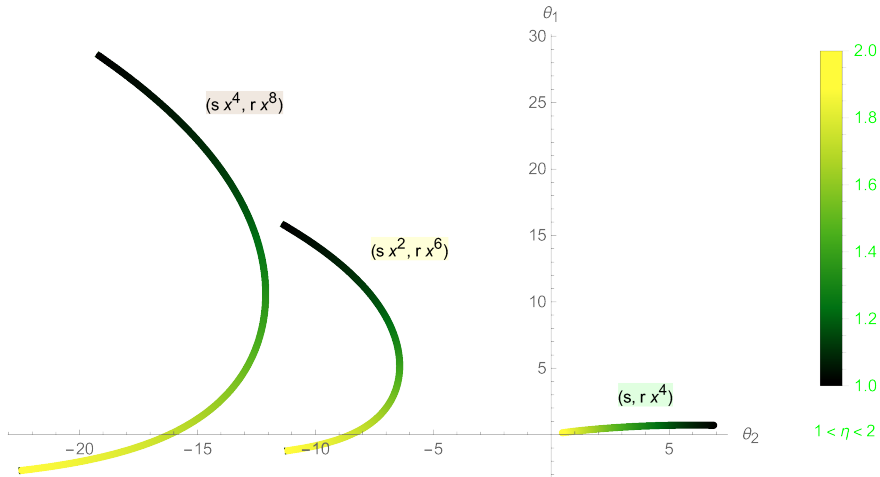


Figure 3: Eigenvalues for three different types of Eigenfunctions:  $(f, h) = \{(s, r x^4), (s x^2, r x^6), (s x^4, r x^8)\}$ , for different values of the anomalous dimension  $1 < \eta < 2$ . The two eigenvalues associated to each value of  $\eta$  within this range, are real and their values are respectively reported on the two axes of the plot.

Remarkably, at  $\eta = 0$ , our numerical determination of the eigenvalue associated with  $q = 4$  (the only one with positive real part), namely  $\theta_{1,2} = 2.919 \pm i 3.923$ , coincides with the eigenvalue of the asymptotically safe trajectory of the Reuter FP found in [17] for the  $R^4$  projection with  $n = +\infty$ .

Finally, in Fig. 3 the eigenvalues in the region  $1 < \eta < 2$  are displayed. In this case, the two complex conjugate solutions found in the other ranges of  $\eta$ , are replaced by two real solutions plotted respectively on the  $x$  and  $y$  axis in the figure. Again, we observe a special role of the solutions with  $q = 4$ , because both real eigenvalues are positive for any value of  $\eta$  in this range. All other solutions, corresponding to  $q > 4$ , have only one positive eigenvalue in the restricted range  $1 < \eta < \bar{\eta}$  (with  $\bar{\eta} \lesssim 2$ ), while the remaining solutions are negative.

Then, we emphasize the striking feature emerging from Figs. 2-3, that at fixed  $\eta$ , all eigenfunctions share the same behavior, with the only exception of the one with  $q = 4$  which, in most cases with complex eigenvalues shows opposite sign of the real part of the eigenvalue with respect to the other eigenfunctions, while it shows at least one eigenvalue with opposite sign, in the case of real eigenvalues.

#### 4. Conclusions

The approximation scheme adopted in this paper to analyze the RG flow of a generalization of the conformally reduced Einstein-Hilbert action, yields a rich picture of the UV critical manifold of the theory.

Specifically, in our approach the background field is treated in the so called single field approximation within the framework of the proper time flow, where the background field is eventually identified with the full field expectation. This scheme implies a distinction between the spectra of  $\hat{\square}$  and  $\bar{\square}$ , and consequently it is possible to introduce the anomalous dimension  $\eta$  through Eqs. (10) and (11), and  $\eta$  is eventually determined by integrating over the fluctuations of the conformal factor.

Then, the generalization of the CREH action reported in Eq. (7), studied in this paper, generates a continuum of fixed points suitably parameterized by the anomalous dimension  $\eta$  in Fig. 1. Each fixed point possesses a discrete spectrum of eigenoperators as shown in Figs. 2 and 3.

On one hand, these findings represent the improvement produced by our approximation scheme with respect to the analysis of the plain CREH truncation [17] where a single FP, namely the Reuter FP related with the property of asymptotic safety, was spotted. On the other hand, the UV critical manifold illustrated here presents an evident dissimilarity with respect to the one derived in [21] where a full background independent approximation scheme (realized by resorting to modified split Ward identities) was adopted and a continuum of fixed points, supporting both a discrete and a continuous eigenoperator spectrum is found. The partial incongruity of the two results, which is certainly to be addressed to the different approaches adopted in the two cases, in our opinion is a clear indicator of the sensitivity of the predictions to the particular procedure and approximation scheme selected.

Turning to the results of the analysis discussed above, if we attempt to establish the physical significance of our solutions from the eigenfunction analysis, rather than from the determination of the sign of the FP shown in Fig. 1, we should discard FPs and eigenfunctions corresponding to  $\eta > 2$ , as in this case we find an infinite number of relevant directions (those with  $q > 4$ ) and just an irrelevant one ( $q = 4$ ) and this would correspond to a not predictive theory.

Conversely, the line of FPs in the range  $\eta < \eta_c \approx 0.96$ , has the desired properties of yielding both positive Newton's Constant and Cosmological Constant, with complex eigenvalues associated to the eigenfunction solutions of the linearized flow equation around each FP, but with just one relevant solution (i.e. with positive real part of the eigenvalue) that produces the renowned spiral behavior. In particular, the FP at  $\eta = 0$  correctly reproduces the main features of the Reuter FP. Moreover,

it is worth noticing that the presence of an endpoint in a continuous line of FPs, analogous to  $\eta_c$  in our analysis, in the case of the two-dimensional Kosterlitz-Thouless transition is directly related to the universal, physically measurable, property of the spin-stiffness jump [28, 29].

Finally, the range  $1 < \eta < 2$  has infinite relevant directions (and therefore it corresponds again to a not predictive theory that must be discarded), except for the small range  $\bar{\eta} < \eta < 2$  where only the two real eigenvalues with  $q = 4$  are positive. Therefore, this small range of  $\eta$  produces a peculiar structure, different from the spiral behavior so far observed, which certainly deserves a more accurate investigation, in order to clarify whether it corresponds to a genuine physical effect and not to an artifact of the adopted approximation.

## Acknowledgements

MC thanks the National Institute of Astrophysics (INAF) section of Catania together with the INAF - Catania Astrophysical Observatory for their hospitality during the preparation of the manuscript. MC acknowledges support from National Institute of Nuclear Physics (INFN). MC also wishes to thank Sergio Cacciatori for his invaluable help with the ‘phiboxing’. This work has been carried out within the INFN project FLAG.

## References

- [1] Roberto Percacci and Daniele Perini. Should we expect a fixed point for Newton’s constant? *Class. Quant. Grav.*, 21:5035–5041, 2004.
- [2] M. Reuter. Nonperturbative evolution equation for quantum gravity. *Phys. Rev. D*, 57:971–985, 1998.
- [3] Robert Percacci. *An Introduction to Covariant Quantum Gravity and Asymptotic Safety*, volume 3 of *100 Years of General Relativity*. World Scientific, 2017.
- [4] Martin Reuter and Frank Saueressig. *Quantum Gravity and the Functional Renormalization Group: The Road towards Asymptotic Safety*. Cambridge University Press, 1 2019.
- [5] Alfio Bonanno, Tobias Denz, Jan M. Pawłowski, and Manuel Reichert. Reconstructing the graviton. *SciPost Phys.*, 12(1):001, 2022.
- [6] Kenneth G. Wilson. Renormalization group and critical phenomena. 1. Renormalization group and the Kadanoff scaling picture. *Phys. Rev. B*, 4:3174–3183, 1971.
- [7] Franz J. Wegner and Anthony Houghton. Renormalization group equation for critical phenomena. *Phys. Rev. A*, 8:401–412, 1973.
- [8] J. F. Nicoll and T. S. Chang. An Exact One Particle Irreducible Renormalization Group Generator for Critical Phenomena. *Phys. Lett. A*, 62:287–289, 1977.
- [9] Joseph Polchinski. Renormalization and Effective Lagrangians. *Nucl. Phys. B*, 231:269–295, 1984.
- [10] Christof Wetterich. Exact evolution equation for the effective potential. *Phys. Lett. B*, 301:90–94, 1993.
- [11] Tim R. Morris. The Exact renormalization group and approximate solutions. *Int. J. Mod. Phys. A*, 9:2411–2450, 1994.
- [12] Tim R. Morris and Dalius Stulga. *The Functional  $f(R)$  Approximation*, pages 1–33. Springer Nature Singapore, Singapore, 2023.
- [13] Abhay Ashtekar and Jerzy Lewandowski. Background independent quantum gravity: A Status report. *Class. Quant. Grav.*, 21:R53, 2004.
- [14] Martin Reuter and Holger Weyer. Background Independence and Asymptotic Safety in Conformally Reduced Gravity. *Phys. Rev. D*, 79:105005, 2009.
- [15] Martin Reuter and Holger Weyer. Conformal sector of Quantum Einstein Gravity in the local potential approximation: Non-Gaussian fixed point and a phase of unbroken diffeomorphism invariance. *Phys. Rev. D*, 80:025001, 2009.
- [16] Pedro F. Machado and R. Percacci. Conformally reduced quantum gravity revisited. *Phys. Rev. D*, 80:024020, 2009.
- [17] Alfio Bonanno and Filippo Guarnieri. Universality and Symmetry Breaking in Conformally Reduced Quantum Gravity. *Phys. Rev. D*, 86:105027, 2012.
- [18] Alfio Maurizio Bonanno, Maria Conti, and Sergio Luigi Cacciatori. Ultraviolet behavior of conformally reduced quadratic gravity. *Phys. Rev. D*, 108(2):026008, 2023.
- [19] Juergen A. Dietz and Tim R. Morris. Background independent exact renormalization group for conformally reduced gravity. *JHEP*, 04:118, 2015.
- [20] Peter Labus, Tim R. Morris, and Zoë H. Slade. Background independence in a background dependent renormalization group. *Phys. Rev. D*, 94(2):024007, 2016.
- [21] Juergen A. Dietz, Tim R. Morris, and Zoe H. Slade. Fixed point structure of the conformal factor field in quantum gravity. *Phys. Rev. D*, 94(12):124014, 2016.
- [22] Alfio Bonanno, Alessandro Codello, and Dario Zappala’. Structural aspects of FRG in quantum tunneling computations. *Annals Phys.*, 445:169090, 2022.
- [23] Alfio Bonanno and Dario Zappala. Towards an accurate determination of the critical exponents with the renormalization group flow equations. *Phys. Lett. B*, 504:181–187, 2001.
- [24] A. Bonanno and M. Reuter. Proper time flow equation for gravity. *JHEP*, 02:035, 2005.
- [25] D. Zappala’. Improving the renormalization group approach to the quantum mechanical double well potential. *Phys. Lett. A*, 290:35–40, 2001.
- [26] Daniel F. Litim and Dario Zappala. Ising exponents from the functional renormalisation group. *Phys. Rev. D*, 83:085009, 2011.
- [27] Tim R. Morris. Elements of the continuous renormalization group. *Prog. Theor. Phys. Suppl.*, 131:395–414, 1998.
- [28] J M Kosterlitz and D J Thouless. Long range order and metastability in two dimensional solids and superfluids. (application of dislocation theory). *Journal of Physics C: Solid State Physics*, 5(11):L124, jun 1972.
- [29] David R. Nelson and J. M. Kosterlitz. Universal jump in the superfluid density of two-dimensional superfluids. *Phys. Rev. Lett.*, 39:1201–1205, Nov 1977.